

---

# A Foundational Dataset for the Predictive Prevention of Waterborne Disease

---

Anonymous Author(s)

Affiliation  
Address  
email

## Abstract

1 We propose the creation of a new, open, and continuous dataset generated by a  
2 global network of autonomous, solar-powered smart buoys. Today, the fight against  
3 waterborne diseases like cholera and typhoid is fundamentally reactive, crippled  
4 by a critical data bottleneck: the lack of timely, high-resolution information on  
5 water quality. Manual sampling is slow, sparse, and expensive, meaning authorities  
6 only learn of a contamination event after people are already sick. By providing  
7 a continuous stream of molecular-level pathogen data fused with environmental  
8 metrics, this dataset will, for the first time, enable the AI community to build  
9 sophisticated, real-time forecasting models for disease outbreaks. Our vision is to  
10 catalyze a global, AI-powered early warning system that transforms public health  
11 from a reactive to a proactive science, preventing outbreaks and saving lives in the  
12 world's most vulnerable communities.

## 13 1 AI Task Definition: Multi-Scale Spatiotemporal Contamination Forecasting

14 The primary AI task is **predictive time-series forecasting and dynamic risk modeling**. The central  
15 scientific question is: *Can we accurately forecast the movement of contaminants and predict the*  
16 *likelihood of a waterborne disease outbreak in a specific location 24-72 hours in advance, based on*  
17 *real-time sensor data and environmental factors?*

18 This overarching goal is composed of three interconnected AI tasks:

- 19 • **Task 1: Time-Series Forecasting of Contaminant Levels.** Given the historical data from  
20 the buoy network, the task is to predict the future concentration of specific pathogens and  
21 pollutants at each sensor location. This is a classic sequence modeling problem well-suited  
22 for state-of-the-art models like **LSTMs, GRUs, and Transformer networks**, which can  
23 capture complex temporal dependencies and seasonalities.
- 24 • **Task 2: Geospatial Risk Mapping and Classification.** This task involves fusing the  
25 time-series predictions with static and dynamic environmental data (e.g., population density,  
26 rainfall anomalies, land use) to classify geographic sub-regions by their immediate outbreak  
27 risk (e.g., low, medium, high). Models like **XGBoost and Random Forest** will be trained  
28 to generate dynamic, hourly-updated risk maps that are intuitive for public health officials.
- 29 • **Task 3: Causal Inference and Driver Analysis.** Beyond prediction, it is critical to  
30 understand *why* an outbreak is likely. The task is to identify the key environmental and sensor-  
31 based factors driving a high-risk prediction. This will be accomplished using **Explainable**  
32 **AI (XAI) techniques like SHAP (SHapley Additive exPlanations)** to interpret model  
33 outputs, providing actionable insights for targeted interventions.

<sup>34</sup> **2 Proposed Dataset Schema:**

<b>Data Stream</b>	<b>Component</b>	<b>Details</b>	<b>Collection Freq.</b>
<b>1. Real-Time Buoy Data</b>	Pathogen Biosensors	Graphene-based biosensors providing molecular-level detection of key pathogens like <i>E. coli</i> , <i>V. cholerae</i> , <i>S. typhi</i> , and chemical fingerprints for pollutants like PFAS.	15-minute intervals
	Water Quality Metrics	Standard multi-modal probes measuring pH, turbidity, conductivity, temperature, and oxidation-reduction potential (ORP).	15-minute intervals
	Geospatial Data	Precise GPS coordinates (latitude, longitude) for each buoy.	15-minute intervals
<sup>35</sup> <b>2. Integrated Contextual Data</b>	Climate & Weather	Precipitation, temperature anomalies, humidity from NASA Giovanni & NOAA archives.	Synced Daily
	Socio-environmental	Population density (NASA SEDAC), land use maps, and infrastructure locations (bridges, industrial sites) to identify pollution sources.	Synced Weekly/Monthly
<b>3. Ground-Truth Labels</b>	Health Surveillance	Anonymized, location-tagged data on confirmed cases of waterborne diseases from partner public health organizations (e.g., PAHO, local Ministries of Health).	Synced as available

<sup>36</sup> **Scale and Scope:** The project will launch with a 200-buoy pilot network in a high-risk watershed  
<sup>37</sup> (e.g., a major river system in a cholera-endemic region). The long-term vision is to scale to thousands  
<sup>38</sup> of units, creating a global, open-source repository for freshwater health.

39 **Appendix**

40 **Alternate Dataset Variation: Fish Scales as Bio-Indicative Tissue Dataset**

41 An alternative approach involves using fish scales as a bio-indicative tissue reflecting environmental  
42 conditions in subsequent growing seasons. In a recent study, fish scales from species such as common  
43 carp (*Cyprinus carpio L.*), chub (*Squalius cephalus*), and nase (*Chondrostoma nasus*) were found to  
44 be highly sensitive to the accumulation of metals like Mn, Ni, and Pb. In some parts of the scales,  
45 concentrations of these metals were up to ten times higher than in the fish's soft tissues, and these  
46 values significantly correlated with metal levels in liver and kidney tissue.

47 This suggests strong potential for developing *colorimetric methods with smartphone analysis* to  
48 detect and quantify such metals via scale-based biosensors.

49 **Analytical Techniques**

- 50 • **X-ray Fluorescence (XRF) and Inductively Coupled Plasma Optical Emission Spec-  
51 trometry (ICP-OES)** have been employed to quantify elements such as Ca, K, Mg, Na, P,  
52 S, Al, Ba, Cu, Cr, Fe, Mn, Sr, and Zn in the scales of species like chub (*Squalius cephalus*)  
53 and nase (*Chondrostoma nasus*), demonstrating significant variability and species-specific  
54 accumulation patterns.
- 55 • **Scanning Electron Microscopy (SEM)** is used to characterize scale morphology, identifying  
56 structural differences that may influence element retention and accumulation.
- 57 • **Micro-XRF Mapping** provides qualitative elemental maps to pre-screen samples before  
58 quantitative ICP-OES analysis, enabling cost-effective sample selection.
- 59 • **Laser-Induced Breakdown Spectroscopy (LIBS)** has shown promise in detecting Fe and  
60 Pb in fish scales (e.g., *Salminus brasiliensis*, *Prochilodus lineatus*), outperforming atomic  
61 absorption spectroscopy in sensitivity—particularly for lead.

62 **Environmental and Structural Insights**

- 63 • Fish scales, as calcareous structures with growth rings, incorporate pollutants over time,  
64 enabling reconstruction of exposure history. Non-lethal sampling and repeated monitoring  
65 are possible.
- 66 • Metal accumulation in scales can occur within days of exposure and often correlates linearly  
67 with ambient water concentrations.
- 68 • Fish fins, like scales, can also bioaccumulate trace metals (e.g., As, Cu, Hg) and in some  
69 cases show correlations with muscle tissue levels, depending on species and metal.

70 **Acceleration Potential: From Reactive Response to Proactive Prevention**

71 This dataset will not be an incremental improvement; it will be a transformational catalyst for public  
72 health, environmental science, and AI research.

- 73 • **For Public Health: Revolutionizing Emergency Response.** Instead of reacting to hospital  
74 reports, health officials can use AI-powered dashboards to receive automated alerts about  
75 high-risk areas. This enables proactive, targeted interventions: distributing water purification  
76 tablets, launching public awareness campaigns, and pre-positioning medical teams *before* a  
77 single person gets sick.
- 78 • **For Environmental Science: A "Digital Twin" for Waterways.** The dataset network will  
79 create the first high-resolution, dynamic map of a river's health. Scientists can use this data  
80 to precisely identify and track pollution sources in real-time and provide policymakers with  
81 the quantitative evidence needed to enforce environmental regulations.
- 82 • **For AI Research: Catalyzing New Algorithmic Frontiers.** dataset will become a bench-  
83 mark dataset for a new class of socio-environmental AI models. It will drive innovation  
84 in:

85           – **Graph Neural Networks (GNNs):** Modeling entire river systems as graphs to predict  
86            how contaminants flow and disperse through the network.  
87           – **Physics-Informed Neural Networks (PINNs):** Integrating the physical laws of fluid  
88            dynamics into deep learning models to improve prediction accuracy.  
89           – **Epidemiology-Aware AI Models (EAAMs):** Developing agent-based models that  
90            simulate human behavior and its interaction with the dynamic contamination map to  
91            forecast disease spread.

92   **Data-Creation Pathway: A Distributed, Autonomous Sensor Network**

93   The data will be generated by a newly designed, open-standard hardware and software platform,  
94   ensuring transparency and community involvement.

95           • **Hardware - The "Smart Buoy":** Each unit is a self-sustaining, low-cost data collection  
96            platform.  
97            – *Sensing:* A modular sensor array featuring novel graphene-based biosensors for  
98            pathogens and standard probes for chemical/physical properties.  
99            – *Power:* A hybrid system using a primary solar panel and secondary energy harvesting  
100            (piezoelectric/triboelectric) from water motion for continuous, long-term, autonomous  
101            operation.  
102            – *Communication:* A low-power, long-range wireless module (e.g., LoRaWAN or cellular  
103            IoT) to transmit data to a central gateway.

104           • **Platform Architecture & Data Flow:**  
105            1. *Ingestion:* Data from the buoy network is transmitted to regional gateways.  
106            2. *Integration & Fusion:* A centralized, cloud-based platform ingests raw sensor data  
107            and automatically fuses it with contextual data streams from NASA, NOAA, and other  
108            archives.  
109            3. *Storage & Access:* The integrated dataset is stored in a time-series database and made  
110            publicly available via a simple, open **API**, ensuring it is FAIR (Findable, Accessible,  
111            Interoperable, and Reusable).

112           • **Deployment Strategy:** We will pursue a phased rollout in partnership with a local river  
113            authority and a public health NGO to ensure the pilot program is grounded in real-world  
114            needs.

115   **Hardware Specifications**

116   Our strategy is designed for cost-effective generation at scale, with a clear path from a pilot project to  
117   a global utility.

118   **Buoy-Based *E. coli* Detection System Overview**

119   The current version of the buoy tested utilizes an optochemical reaction that changes color in the  
120   presence of *E. coli*, with a camera mounted on top to capture and relay the visual information. The  
121   system involves two main vials used for the biochemical detection of coliforms.

122   **First Vial: Lauryl Tryptose Broth (LTB) Powder**

123   This vial contains a dehydrated powder formulation of Lauryl Tryptose Broth, designed to be  
124   reconstituted with 10 mL of water obtained from a pre-concentrated 100 mL water sample. The  
125   standard composition per liter of LTB is:

126   Final pH:  $6.8 \pm 0.2$  at 25°C.

127   **Function:** This medium is commonly used for the detection of coliform bacteria in water and food  
128   samples.

Component	Concentration (g/L)
Tryptose	20.0
Lactose	5.0
Sodium Chloride (NaCl)	5.0
Dipotassium Hydrogen Phosphate (K <sub>2</sub> HPO <sub>4</sub> )	2.75
Potassium Dihydrogen Phosphate (KH <sub>2</sub> PO <sub>4</sub> )	2.75
Sodium Lauryl Sulfate (SLS)	0.1

129 **Second Vial: Gel-Based Detection Matrix**

130 This vial contains a gel matrix (100–1000 µL) composed of the following:

- 131 • **Agar or Purified Agar:** 2–20 mg  
132 Serves as a gelling agent to provide structural integrity.
- 133 • **Triton X-100 in Tris-HCl Buffer (10–50 mM, pH 7.5–8.5):** 25–100 µL  
134 Triton X-100 is a non-ionic surfactant that lyses cells, releasing intracellular enzymes.  
135 Tris-HCl buffer maintains pH stability.
- 136 • **Lauryl Tryptose Broth Solution:** 100–400 µL  
137 Provides nutrients to support coliform bacterial growth during incubation.
- 138 • **Chemical Solution/Mixture:** 50–200 µL, containing:
  - 139 – **6-Chloro-3-indolyl-β-D-galactopyranoside (Red-Gal):** 20–90 mg  
140 A chromogenic substrate for β-galactosidase. Upon enzymatic cleavage, a colored  
141 product is formed, enabling visual detection.
  - 142 – **N,N-Dimethylformamide (DMF):** 1000–2000 µL  
143 Solvent for Red-Gal, which is sparingly soluble in water.
  - 144 – **Deionized Water:** 1000–2000 µL  
145 Used to dilute the chemical mixture to the desired concentration.

146 **Function:** This matrix visually indicates coliform presence by detecting β-galactosidase activity,  
147 which cleaves Red-Gal to produce a colored compound.

148 **Data Processing and Transmission**

149 An edge-computing microcontroller processes sensor data and transmits it via a LoRaWAN/IoT  
150 network. Collected data is streamed to an online system for real-time processing and visualization as  
151 an AI-assisted geospatial contamination map.

152 **Additional Features:**

- 153 • Parameters such as turbidity, pH, conductivity, and oxidation-reduction potential (ORP) are  
154 simultaneously recorded.
- 155 • The AI model analyzes this dataset to predict contamination hotspots and pollutant dispersion  
156 patterns along the river's path through villages, urban centers, and industrial zones.

157 **Proposed Biosensor Methodology**

158 The next step is to create biosensors via the immobilization of enzymes that target analytes released  
159 during the respiration of *Salmonella*, *Shigella*, *Cholera*, and *E. coli*. When these bacteria respire,  
160 they produce analytes that, upon contacting specific enzymes, generate a varying electric current  
161 measurable with an ammeter to determine bacterial presence.

162 Graphene on a plastic film is submerged in a 5 mM solution of 1-pyrenebutyric acid (PBA) dissolved  
163 in DMSO and left at room temperature. After two hours, the substrates are removed and rinsed with  
164 distilled water, bonding the PBA onto the graphene through π-π interactions.

165 **Enzyme immobilization:** Glucose Oxidase, Glycerol-3-Phosphate Oxidase, Galactose Oxidase, and  
166 Lactate Oxidase are immobilized onto the PBA-functionalized graphene. First, 24 µL of distilled

167 water is added to the anhydrous enzyme, and the solution is ultrasonicated for 180 s. This process is  
168 repeated for each enzyme. One aliquot of each enzyme is micro-pipetted onto a separate graphene  
169 substrate and stored at 7 °C overnight to complete immobilization.

170 Conductive paint terminals are applied on opposite, parallel sides of the graphene biosensor to  
171 facilitate electrical measurements.

## 172 Sensor for PFAS Detection

173 The sensor is built on a **lateral-flow paper-based platform**—a format similar to that used in  
174 COVID-19 and pregnancy tests. Unlike antibody-based visual readouts, this sensor uses a **conductive**  
175 **polymer** to detect PFAS (per- and polyfluoroalkyl substances) through changes in electrical resistance.

## 176 Core Technical Components

### 177 Polymer: Polyaniline

178 The active sensing element is **polyaniline**, a conductive polymer that can reversibly switch between  
179 semiconducting and conducting states when protons interact with it.

### 180 Substrate: Nitrocellulose Paper

181 Polyaniline is deposited onto a **nitrocellulose strip**, which acts as a structural substrate. This material  
182 allows for **fluid wicking** and ensures the platform remains lightweight and portable.

### 183 Surfactant Coating

184 A **surfactant layer** coats the strip and facilitates the extraction of **acidic PFAS molecules**, including:

- 185 • PFOA (Perfluorooctanoic acid)
- 186 • PFBA (Perfluorobutanoic acid)

187 These molecules are drawn from a small droplet of water into the sensing region.

## 188 Detection Mechanism

### 189 PFAS-Driven Proton Transfer

190 When acidic PFAS enter the sensor strip, **protons are transferred into the polyaniline**, switching it  
191 from a semiconducting to a conducting state. This transition causes a **drop in electrical resistance**,  
192 which forms the basis for detection.

### 193 Quantitative Readout

194 **Electrodes** embedded in the device measure the change in resistance, yielding a quantitative signal  
195 that corresponds to the PFAS concentration. This electrical signal can be:

- 196 • **Read via an ammeter**
- 197 • **Transmitted to a smartphone** or external device for data processing and display



Figure 1: Proposed Buoy System

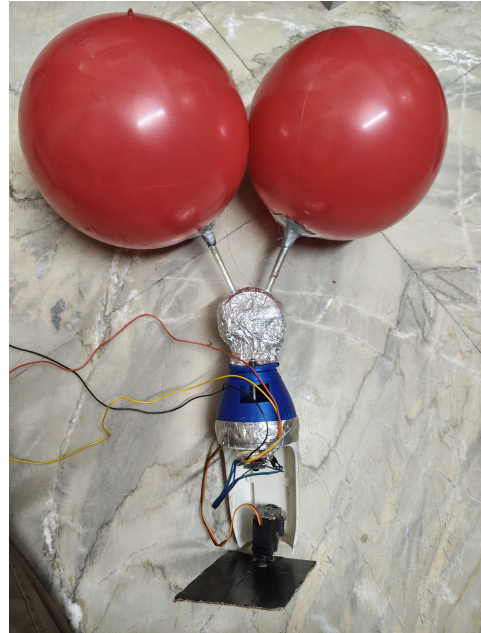


Figure 2: Early prototype version carrying the red-gal chemical test for e.coli

## 198 References

- 199 1 United Nations Environment Programme. (2021, March 22). Globally, 3 billion people at health risk due to scarce data on water quality.  
200 UNEP News. <https://www.unep.org/news-and-stories/story/globally-3-billion-people-health-risk-due-scarce-data-water-quality>
- 201 2 World Health Organization. (2022, March 22). Drinking-water. WHO Fact-sheet on Global Water Contamination. <https://www.who.int/news-room/fact-sheets/detail/drinking-water>
- 202 3 World Bank. (2025, February 28). World Water Day: Two billion people still lack access to safely managed water. <https://blogs.worldbank.org/en/opendata/world-water-day-two-billion-people-still-lack-access-safely-managed-water>
- 203 4 Shah, A., Arjunan, A., Baroutaji, A., & Zakharova, J. (2023). A review of physicochemical  
204 and biological contaminants in drinking water and their impacts on human health. *Water  
205 Science and Engineering*, 16(4), 333–344. <https://doi.org/10.1016/j.wse.2023.04.003>
- 206 5 SIWI. (2017, August 30). Ryan Thorpe and Rachel Chang  
207 from the USA win 2017 Stockholm Junior Water Prize. *Stockholm  
208 International Water Institute*. <https://siwi.org/latest/ryan-thorpe-rachel-chang-usa-win-2017-stockholm-junior-water-prize/>
- 209 6 Odobašić, A., Šestan, I., & Begić, S. (2019). Biosensors for determination of heavy metals  
210 in waters. *IntechOpen*. <https://doi.org/10.5772/intechopen.84139>
- 211 7 Hassan, M., Zhao, Y., & Zughaiyer, S. M. (2024). Recent advances in bacterial detection  
212 using surface-enhanced Raman scattering. *Biosensors*, 14(8), 375. <https://doi.org/10.3390/bios14080375>
- 213 8 Payne, T. D., Klawan, S. J., Jian, T., Wang, Q., Kim, S. H., Freeman, R., & Schultz, Z.  
214 D. (2023). From the lab to the field: handheld surface enhanced Raman spectroscopy  
215 (SERS) detection of viral proteins. *Sensors & diagnostics*, 2(6), 1483–1491. <https://doi.org/10.1039/d3sd00111c>
- 216 225

226 9 Chen, S.-E., Yang, R.-Y., Qiu, Z.-H., & Wu, C.-C. (2021). A Piezoelectric Wave Energy  
227 Harvester Using Plucking-Driven and Frequency Up-Conversion Mechanism. *Energies*,  
228 14(24), 8441. <https://doi.org/10.3390/en14248441>

229 10 Xie, X. D., Wang, Q., & Wu, N. (2014). Energy harvesting from transverse ocean waves  
230 by a piezoelectric plate. *International Journal of Engineering Science*, 81, 41–48. <https://doi.org/10.1016/j.ijengsci.2014.04.003>

231 11 Nasr, N., Shafi, M., Zhao, T., Ali, R., Ahmad, I., Khan, M., Deifalla, A., Ragab, A. E.,  
232 & Ansari, M. Z. (2024). A two-fold SPR-SERS sensor utilizing gold nanoparticles and  
233 graphene thin membrane as a spacer in a 3D composite structure. *Spectrochimica Acta Part*  
234 *A: Molecular and Biomolecular Spectroscopy*, 304, 123331. <https://doi.org/10.1016/j.saa.2023.123331>

235 12 Wei, Q., Nagi, R., Sadeghi, K., Feng, S., Yan, E., Ki, S. J., Caire, R., Tseng, D., & Ozcan,  
236 A. (2014). Detection and spatial mapping of mercury contamination in water samples  
237 using a smart-phone. *ACS Nano*, 8(2), 1121–1129. <https://doi.org/10.1021/nn406571t>

238 13 Marie Adier, Anne-Marie Jurdyc, Charlotte Hurel, François Goutaland, Jean-Yves Michalon,  
239 et al. (2023). Toward surface-enhanced Raman scattering using electroless substrate  
240 for trace arsenic detection and speciation. *Journal of Applied Physics*, 133(7), 073103.  
241 <https://doi.org/10.1063/5.0126372>

242 14 Park, S., Gordon, C.T., & Swager, T.M. (2024). Resistivity detection of perfluoroalkyl  
243 substances with fluorous polyaniline in an electrical lateral flow sensor. *Proceedings of the*  
244 *National Academy of Sciences*, 121(12), e2317300121. <https://doi.org/10.1073/pnas.2317300121>

245 15 Viana, L. F., Súarez, Y. R., Cardoso, C. A. L., Lima, S. M., da Cunha Andrade, L. H., &  
246 Lima-Junior, S. E. (2019). Use of fish scales in environmental monitoring by the application  
247 of Laser-Induced Breakdown Spectroscopy (LIBS). *Chemosphere*, 228, 258–263. <https://doi.org/10.1016/j.chemosphere.2019.04.070>

248 16 Marić, B., Rašković, B., Babović, N., Hegediš, A., Spasić, M., Lenhardt, M., & Poleksić,  
249 V. (2023). Prospects of fish scale and fin samples usage for nonlethal monitoring of  
250 trace element contamination in freshwater fish. *Knowledge and Management of Aquatic*  
251 *Ecosystems*, 424, 12. <https://doi.org/10.1051/kmae/2023010>

252 17 Varga, M., Szakál, A., Kálmán, E., Harangi, S., Baranyai, E., & Nagy, S. A. (2025). Fish  
253 Scales as a Non-Invasive Method for Monitoring Trace and Macroelement Pollution in  
254 Rivers. *Animals*, 15(6), 943. <https://doi.org/10.3390/ani15060943>

255 18 Vaid, V., & Hundal, S. S. (2024). Ultrastructural Studies to Evaluate Fish Scales as Indicators  
256 of Heavy Metals in *Labeo rohita*. *Journal of Soil Salinity and Water Quality*, 16(1), 89–96.  
257 <https://doi.org/10.56093/JSSWQ.v16i1.148991>

258 19 Jain, S., Chattopadhyay, S., Jackeray, R., Abid, C. K. V. Z., Kohli, G. S., & Singh, H.  
259 (2017). DipTest: A litmus test for *E. coli* detection in water. *PLoS ONE*, 12(9), e0183234.  
260 <https://doi.org/10.1371/journal.pone.0183234>

261 20 Mallmann, W. L., & Darby, C. W. (1941). A new medium for the enumeration of coliform  
262 organisms. *American Journal of Public Health*, 31(2), 127–132. <https://doi.org/10.2105/AJPH.31.2.127>

263 21 Li, Y., Wang, Z., Sun, L., Liu, L., Xu, C., & Kuang, H. (2019). Colorimetric Detection  
264 of *Escherichia coli* Based on the Enzyme-Induced Metallization of Gold Nanorods. *ACS*  
265 *Applied Materials Interfaces*, 11(46), 43382–43389. <https://doi.org/10.1021/acsami.9b16758>

266 22 Earthface Private Limited. (2025). Padma Bio: *E. coli* Water Testing Kit [Product informa-  
267 tion]. <https://www.earthface.in/product/padma-bio>

268

269

270

271

272

273

274